4. S.-H. Chen, *Annu. Rev. Phys. Chem.* **37**, 351 (1986).
5. J. M. Haile and J. P. O'Connell, *J. Phys. Chem.* **88**, 6363 (1984).
6. M. C. Woods *et al.*, *ibid.* **90**, 1875 (1986).
7. B. Jonsson *et al.*, *J. Chem. Phys.* **85**, 2259 (1986).
8. K. Watanabe *et al.*, *J. Phys. Chem.* **92**, 819 (1988).
9. M. Elder, P. Hitchcock, R. Mason, C. G. Shipley, *Proc. R. Soc. London Ser. A* **354**, 157 (1977).
10. K. A. Dill and P. J. Flory, *Proc. Natl. Acad. Sci. U.S.A.* 77, 3115 (1980).
11. ——, *ibid.* **78**, 676 (1981).
12. K. A. Dill *et al.*, *Nature* **309**, 42 (1984).
13. K. A. Dill and R. S. Cantor, *Macromolecules* **17**, 380 (1984).
14. T. Zemb and C. Chachaty, *Chem. Phys. Lett.* **88**, 68 (1982).
15. B. Owenson and L. R. Pratt, *J. Phys. Chem.* **84**, 2906 (1984).
16. J. P. Bareman, G. Cardini, M. L. Klein, *Phys. Rev. Lett.* **60**, 2152 (1988).
17. I. Szleifer *et al.*, *J. Chem. Phys.* **85**, 5345 (1986).
18. ——, *ibid.* **83**, 3612 (1985).
19. W. L. Jorgensen *et al.*, *ibid.* **79**, 926 (1983).
20. P. Weiner and P. A. Kollman, *J. Comput. Chem.* **2**, 287 (1981).
21. S. J. Weiner *et al.*, *J. Am. Chem. Soc.* **106**, 765 (1984).
22. B. R. Brooks, in *Supercomputer Research in Chemistry and Chemical Engineering*, C. Jensen and D. Truhlar, Eds. (American Chemical Society, Washington, DC, 1987), pp. 123–145.
23. We thank Z. Wasserman for analysis code development and R. Hilmer for computer graphics code (MOLEDITOR). C.E.S. thanks the American Heart Association and NIH for partial support.

17 August 1988; accepted 23 November 1988

Critical Depth for the Survival of Coral Islands: Effects on the Hawaiian Archipelago

RICHARD W. GRIGG AND DAVID EPP

Coral islands drown when sea level rise exceeds the maximum potential of coral reefs to grow upward (about 10 millimeters per year). During the Holocene transgression (18,000 years ago to present) sea levels rose at rates of up to 10 to 20 millimeters per year, and most coral island reefs situated deeper than a critical depth of 30 to 40 meters below present day sea level drowned. Coral islands that did not drown during the Holocene transgression apparently all developed on antecedent foundations shallower than critical depth. During low stands in sea level during the Pleistocene, these islands were elevated and subject to subaerial erosion. Today, in the Hawaiian Archipelago, the depth of drowned banks is inversely related to summit area; smaller banks are progressively deeper, evidently because of erosional truncation during low sea level stands. Bank summit area may therefore be an important factor determining the failure or success of coral islands.

THE FORMATION OF CORAL ATOLLS has been generally understood since the work of Darwin (*1*). In Darwin's theory, a coral reef grows upward around a sinking volcano until the volcanic edifice subsides below sea level, leaving a coral atoll. However, among 261 atolls in the world's oceans, there are 116 drowned shallow banks, all suitable for the development of atolls (*2, 3*). Many of these banks have the shape of atolls and are at depths between 10 and 200 m. Why these banks drowned while others adjacent or nearby did not has been a long-standing question (*2, 4, 5*). In several atoll-guyot pairs, for example, Bikini and Sylvania, one edifice drowned and the other did not (*6, 7*). Schlager (*8*) has described the problem of reef drowning as a paradox because he suggested that the growth potential of reefs is capable of exceeding the rate of postglacial sea level rise. In this report, we redefine the problem, claiming that during cycles of glacio-eustacy, coral reefs that are situated on banks below a critical depth drown, but reefs growing on shallower foundations do not. We hypothesize that bank depth depends primarily on subaerial erosion which in turn depends on bank summit area and sea level history. We have tested this hypothesis against a set of data from drowned banks in the Hawaiian Archipelago.

The Hawaiian Archipelago is an ideal setting for the study of drowned coral reefs. The chain stretches west-northwest across the Pacific between 20°N and 29°N, from the island of Hawaii to Kure atoll, and contains eight high volcanic islands, five islets with broad banks, three atolls, two coral islands at sea level, and 25 drowned banks (Fig. 1). All of these edifices originated over a hotspot currently located near 19°N 155°W (*9, 10*). Although the archipelago is in tropical latitudes suitable for the development of coral reefs (*11*), some banks have drowned while others have not.

Processes contributing to changes in depth of coral reefs include reef growth, change in eustatic sea level, erosion, and subsidence or uplift of antecedent foundations (Tables 1 and 2). Coral reefs drown when sea level rise outpaces the rate of carbonate accumulation, minus subsidence and erosion, for periods long enough that reefs submerge below a "critical depth." Below this depth, coral reefs cannot maintain a positive net rate of upward accretion.

Sea level has undergone at least 17 cycles of transgression and regression during the Pleistocene (*12, 13*), all likely constrained within several tens of meters above and about 200 below present sea level (*14*). Most workers have estimated that the last sea level low stand in the Holocene was 120 to 135 m below present sea level (*13, 15–17*) (Fig. 2), but it may have been as much as 165 m lower (*18*). Between 18,000 and 9,000 years ago, the long-term average sea level rise was about 12 mm/year (*8, 14*); however, the rise may have been up to 20 mm/year during intervals spanning several thousand years (*18, 19*).

For comparison, maximum rates of net upward coral reef growth are generally about 10 mm/year or less (*13, 20–22*) (Table 1). Higher rates have been measured for maximum potential growth of corals in optimal environments (*23, 24*), but these are not representative of entire reefs. Highest rates of calcification for corals (and reefs) occur at depths of 5 to 10 m and decline rapidly with increasing depth (*25, 26*). At 30 m, rates of vertical growth of individual species of massive corals are between 15 and 40% of their rates at optimum depth (*24–26*). For example, in Jamaica, the rate of upward accretion of the entire reef at 30 m is 1.3 mm/year; about 20% of the rate at 10 m (*25, 27*). This low rate of carbonate production is close to average rates of biological and mechanical erosion (Table 2). Thus rates of sea level rise during the height of the Holocene transgression were greater than the maximum potential of coral reefs to grow upward, particularly if rates of erosion and subsidence are taken into account (Tables 1 and 2).

The critical depth for drowning for most coral reefs in the world is estimated to be about 30 to 40 m, but could be less depending on geographic differences in ecological factors such as light, temperature, sedimentation, turbidity, disturbance, and bioerosion (*8*). Darwin (*1*) recognized the significance of critical depth and called it the limit of vigorous growth. He placed it at a depth of 36 m. Vaughan and Wells (*28*) estimated the zone of vigorous growth to be less than 30 m. Buddemeier and Hopley (*29*) placed it at 40 m. Geologists, in many cases, have estimated that critical depth is deeper; between 50 and 100 m (*8, 30*). Deep-water coral species may survive at depths much greater than 40 m (*13, 31*) but entire reefs below this depth are generally unable to

R. W. Grigg, Hawaii Institute of Marine Biology, University of Hawaii, Honolulu, HI 96822.
D. Epp, National Science Foundation, 1800 G Street, NW, Washington, DC 20550.

build to the surface. Schlager (*8*) equated critical depth for coral reefs with the bottom of the euphotic zone, at a depth of 100 m; he suggested that submergence by 100 m would not cause drowning because successive glacio-eustatic falls would re-expose such reefs. Successive exposure has probably occurred, but because critical depth for coral reefs is much shallower than 100 m, these reefs would simply undergo repeated drownings and would not survive.

In Hawaii, maximum rates of net reef growth at 10 m depth vary between 10 and 1 mm/year, decreasing with increasing latitude (*11*). All drowned Hawaiian banks are in the northwestern Hawaiian Islands (NWHI) between 23° and 29°N where values of net reef growth on adjacent islands at 10 m depth are from 5.0 to less than 1.0 mm/year (*11*). At 30 m depth, accretion rates would be expected to be about one-fifth the rate at 10 m, about 1.0 to less than 0.2 mm/year in the NWHI. These rates of coral reef accretion are much less than the maximum rate of sea level rise during the Holocene.

About 18,000 years ago, most present-day atolls and coral islands were elevated 100 m or more above sea level (*3, 21, 32–34*). The primary evidence that these islands were exposed is a worldwide solution unconformity underlying many coral islands in tropical seas today. This unconformity occurs at depths between 3 and 33 m and separates Holocene reefs from their Pleistocene or younger foundations (*21, 35*). At Enewetak the unconformity occurs at a depth of 10 to 14 m and separates reefs that are 6,000 years old from those that are about 120,000 years old (*36*). At Muroroa in the Tuamoto Islands the same unconformity is at 6 to 10 m depth (*37*). On the Great Barrier Reef the unconformity occurs at depths between 4 and 23 m (*13, 21*). It occurs as deep as 33 m in the Alacran reef, off the east coast of Mexico (*35*). Regional differences in depth of this unconformity may be attributed to varying rates of erosion, as well as subsidence associated with tectonic effects, such as volcanic loading or variable thermal subsidence of the underlying lithosphere (Table 2).

If growth rates of coral reefs in the NWHI are much less than rates of Holocene sea level rise, why are any islands in the NWHI at sea level? A possible explanation is that Kure, Midway, Pearl and Hermes, Lisianski, and Laysan islands and French Frigate Shoals all have shallow Pleistocene foundations that are now above critical depth at their latitudes. Because coral reef growth rates decrease to the north along the chain (*11*), critical depth should decrease to the north. About 10,000 years ago sea level was about 30 m lower than it is today (*17, 38*), and since that time, it has risen at an average rate of only 3 mm/year. Thus if the southerly banks were at depths of 30 m or less, they might have kept pace with sea level, but those in the north would have required shallower foundations to avoid drowning. This hypothesis is readily testable by drilling in the present coral islands in the NWHI.

Table 1. Rates of coral reef growth in three oceans of the world; I, Island; VI, Virgin Islands.

Area	Rate (mm/year)	Reference
Atlantic Ocean		
St. Croix, U.S. VI	9 to 15	(*17*)
Alacran, Mexico	Up to 12	(*35*)
Caribbean	1 to 12	(*21*)
St. Croix, U.S. VI	4 to 10	(*42*)
Bermuda	1 to 3*	(*43*)
Jamaica	1.3	(*27*)
Pacific Ocean		
Hawaii	1 to 10	(*11*)
Eastern Pacific	About 10	(*20*)
Hawaii and Johnson I	Up to 9	(*44*)
Australia	Up to 8	(*21*)
Australia	2.6 to 7.3	(*13*)
Australia	1.5*	(*21*)
Indian Ocean		
Mauritius	Up to 10	(*45*)

*Growth by sedimentation.

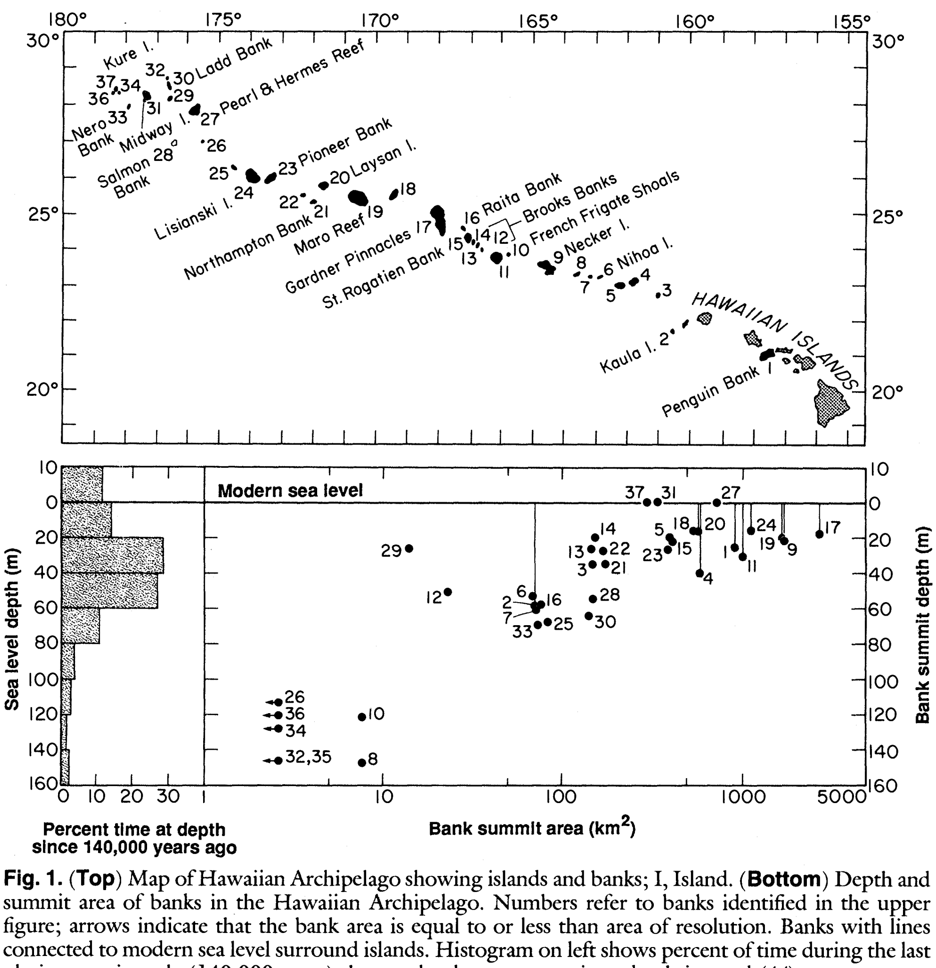

Fig. 1. (**Top**) Map of Hawaiian Archipelago showing islands and banks; I, Island. (**Bottom**) Depth and summit area of banks in the Hawaiian Archipelago. Numbers refer to banks identified in the upper figure; arrows indicate that the bank area is equal to or less than area of resolution. Banks with lines connected to modern sea level surround islands. Histogram on left shows percent of time during the last glacio-eustatic cycle (140,000 years) that sea level was at any given depth interval (*14*).

Measurements of the depth and area of drowned banks in tropical seas provide additional data for interpreting critical depth of coral reefs. We determined the summit depths of banks less than 200 m deep in the NWHI as the shallowest flat surface area exceeding 1.0 km^2 (*39*). The summit area of the drowned banks was determined as the area enclosed within the 180 m (100 fathom) contour. Banks deeper than 200 m are guyots (*40*) and were not considered in the study.

The data show that banks with smaller summit areas are progressively deeper (Fig. 1, bottom). The logarithm of bank summit area is inversely related to depth. With one exception (Salmon Bank) the largest banks in the archipelago (>147-km^2 summit area) all cluster in a depth range of 16 to 40 m. With one exception (Gambier Shoal), middle size bank summits (147 to 10 km^2) are at depths between 51 and 69 m. Banks less than 10 km^2 in summit area are all at depths of 114 to 148 m.

During the past 140,000 years (Fig. 1, bottom) sea level was below 80 m for less than 20% of the time and below 100 m for only 10% of the time (*13*). This period represents only the last glacio-eustatic cycle but is probably typical of sea level cycles during the entire Pleistocene (*13, 14*). If so, the cumulative time sea level has been below 100 m during the entire Pleistocene would be about 160,000 years.

Menard (*40*) determined that the rate of horizontal erosion of volcanic islands attributed to wave action is 0.6 to 1.7 km per million years (Table 2). For a mean of this rate (1.15 km per million years) and if erosion is radial and equal on all sides of an island, only islands smaller than about 0.4 km in diameter would be truncated below 100 m in 160,000 years. The diameter of banks deeper than 100 m in the NWHI is ≤1.8 to 3.1 km. For Menard's rate for horizontal erosion, truncation of these pedestals would require about 0.8 to 1.3 million years, at least five times as much time as sea level spent at 100 m or greater depths during the Pleistocene (Fig. 1, bottom). This discrepancy may indicate that Menard's erosion rate is low, or more likely, that these banks were eroded during low sea level stands in the Pliocene and Miocene (*41*). On

Table 2. Rates of sea level rise, reef erosion, and subsidence of volcanic foundations and causal mechanisms.

Cause	Rate (mm/year)	Reference
Sea level rise		
Holocene transgression	Up to 20	(*19*)
Holocene transgression	Up to 17	(*23*)
Holocene transgression	Up to 15	(*18*)
Holocene transgression	Up to 15	(*15*)
Holocene transgression	Up to 14	(*46*)
Holocene transgression	Up to 12	(*14*)
Holocene transgression	Up to 10	(*8*)
Holocene transgression	Up to 8	(*17*)
Desiccation of oceans	Up to 10	(*47*)
Seafloor spreading	0.01	(*8*)
Midplate volcanism	0.02	(*48*)
Antarctic ice surge	Up to 7	(*49*)
Reef erosion		
Biocrosion	Up to 9.11	(*21*)
Intertidal mechanical, biological, and chemical erosion	0.5 to 1.0	(*50*)
All forms of erosion for entire reefs	0.05 to 4.0	(*21*)
Range of erosion in Grand Cayman Island	0.45 to 2.77	(*51*)
Wave truncation	0.6 to 1.7	(*40*)
Subsidence		
Volcanic loading		
Hawaii	2.7	(*30*)
Lanai	1.7	(*52*)
Midway	0.02	(*21*)
Koko guyot	0.04	(*53*)
Enewetak	0.02 to 0.04	(*21*)
Lithospheric cooling	0.10 to 0.35	(*54*)
	0.01	(*40*)
Seafloor spreading	0.01	(*55, 48*)
Loading from coral growth	0.02 to 0.20	(*21*)

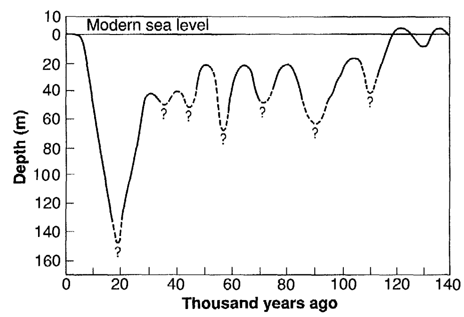

Fig. 2. Depth of sea level during the last 140,000 years (*16*).

the basis of extrapolation from dated islands in the Hawaiian Archipelago, all banks in the NWHI are Pliocene or older in age. Although sea level depth history during the Pliocene and Miocene is not known with sufficient accuracy to allow the development of detailed models of insular erosion for individual banks, the inverse relation between bank summit area and bank depth and the flat-topped morphology of the banks suggests that all were truncated by wave erosion.

Thus small banks should be truncated faster and hence to greater depth than large banks. Deeper banks are more likely to drown than shallow banks because below the critical depth, coral reef accretion cannot keep pace with high rates of sea level rise. The problem of the origin of paired living and dead atolls (7) may be explained simply as a difference in size; the smaller dead guyot was truncated at an ancient sea level low stand and drowned while the larger edifice resisted erosion and was able to support a growing coral reef during subsequent changes in sea level because it could continually provide an edifice above critical depth. This explanation is supported by the size and depth of basaltic foundations underlying two atoll-guyot pairs in the Marshall Islands (Bikini-Sylvania and Mili-Harrie). The basalt foundations of Sylvania and Harrie are both smaller and deeper than the adjacent atoll (7).

Thus the success or failure of coral islands appears to depend on the depth of antecedent foundations relative to critical depth and sea level rise. Carbonate banks above critical depth survive, those below, drown. Hence, drowning is not a paradox (*8*). During the first half of the Holocene transgression (18,000 to 9,000 years ago) sea level rise outpaced the ability of all reefs in the world submerged below critical depth (30 to 40 m or less) to build upward. During the height of the transgression, even reefs growing at maximum rates (10 mm/year) would have deepened by 10 m in 1000 years and would have fallen below critical depth in 3000 to 4000 years. Today in the NWHI drowned banks with smaller summit area are progressively deeper, evidently the result of truncation during periods of low sea level: Bank summit area may therefore be an important factor determining the success or failure of coral islands.

REFERENCES AND NOTES

1. C. Darwin, *The Structure and Distribution of Coral Reefs* (Univ. of California, Press, Berkeley and Los Angeles, 1962).
2. H. W. Menard, *J. Geophys. Res.* **89**, 11117 (1984).
3. ———, *Islands* (Scientific American, New York, 1986).
4. A. L. Bloom, *Soc. Econ. Paleontol. Mineral. Spec. Pub.* **18**, 1 (1974).
5. J. F. Campbell, *Geo-Mar. Lett.* **4**, 31 (1984).
6. K. O. Emery, J. I. Tracy, Jr., H. S. Ladd, *U.S. Geol. Surv. Prof. Pap. 206A* (1954).
7. S. O. Schlanger, in *Report of the Workshop on Carbonate Banks and Guyots*, U.S. Science Advisory Committee, E. L. Winterer and W. Schlager, Eds. (1986), pp. M1–M25.
8. W. Schlager, *Geol. Soc. Am. Bull.* **92** 197 (1981); P. Hallock and W. Schlager, *Palaios* **1**, 389 (1986).
9. J. T. Wilson, *Can. J. Phys.* **41**, 863 (1963).
10. W. J. Morgan, *Am. Assoc. Petrol. Geol. Bull.* **56**, 203 (1972).
11. R. W. Grigg, *Coral Reefs* **1**, 29 (1982).
12. G. J. Kukla, *Earth Sci. Rev.* **13**, 307 (1977).
13. D. Hopley, *The Geomorphology of the Great Barrier Reef: Quaternary Development of Coral Reefs* (Wiley, New York, 1982).
14. J. Chappell, in *Perspectives on Coral Reefs*, D. J. Barnes, Ed. (Australian Institute Marine Science, Manuka, Australia, 1983), pp. 38–55.
15. A. L. Bloom *et al.*, *Quat. Res.* **4**, 185 (1974).
16. J. Chappell and H. A. Polach, *Geol. Soc. Am. Bull.* **87**, 235 (1976).
17. W. H. Adey, *Science* **202**, 831 (1978).
18. H. H. Veeh and J. J. Veerers, *Nature* **226**, 536 (1970).
19. A. L. Bloom, in *The Late Cenozoic Glacial Ages*, K. Turekian, Ed. (Yale Univ. Press, New Haven, 1971), pp. 355–379.
20. P. Glynn and I. G. Macintyre, in *Proceedings of the Third International Coral Reef Symposium*, D. L. Taylor, Ed. (Univ. of Miami, Miami, 1977), p. 251.
21. P. J. Davies, in *Perspectives on Coral Reefs*, D. J. Barnes, Ed. (Australian Institute Marine Science, Manuka, Australia, 1983), pp. 69–106; S. T. Trudgill, *Z. Geomorphol. Suppl.* **26**, 164 (1976).
22. R. W. Buddemeier and S. V. Smith, *Coral Reefs* **7**, 51 (1988).
23. K. E. Chave *et al.*, *Mar. Geol.* **12**, 123 (1972).
24. R. W. Buddemeier, J. E. Maragos, D. K. Knutson, *J. Exp. Mar. Biol. Ecol.* **14**, 179 (1974).
25. P. Dustan, *Mar. Biol.* **33**, 101 (1975).
26. P. A. Baker and J. N. Weber, *Earth Plan. Sci. Lett.* **27**, 57 (1975).
27. T. F. Goreau and L. S. Land, in *Reef Symposium Special Publication* (Society of Economic Paleontologists and Minerologists, Calgary, Canada, 1973), pp. 1–10.
28. T. W. Vaughan and J. Wells, *Geol. Soc. Am. Spec. Pap.* **44**, 1 (1943).
29. R. W. Buddemeier and D. Hopley, in *Proceedings of the Sixth International Coral Reef Symposium*, Townsville, Australia, 8 to 13 August 1989 (in press).
30. B. J. Szabo and J. G. Moore, *Geology* **14**, 967 (1986).
31. J. E. Maragos, *Pac. Sci.* **28**, 257 (1974).
32. E. G. Purdy, *Soc. Econ. Palentol. Minerol. Spec. Pub.* **18**, 9 (1974).
33. CLIMAP Project Members, *Science* **191**, 1131 (1976).
34. J. M. Lincoln and S. O. Schlanger, *Geology* **15**, 454 (1987).
35. I. G. Macintyre, R. B. Burke, R. Stuckenrath, *ibid.* **5**, 649 (1977).
36. D. L. Thurber, W. S. Broecker, R. L. Blanchard, H. A. Potratz, *Science* **149**, 55 (1965).
37. C. Lalou, J. Labeyrie, G. Delebrias, *Acad. Sci. Compte Rendus Hebdomadaires Seances. Ser. D* **263**,

1946 (1966).
38. A. C. Neumann and I. Macintyre, in *Proceedings Fifth International Coral Reef Congress*, B. Delesalle, R. Galzin, B. Salvat, Eds. (Ant. Museum-Ephe, Moorea, French Polynesia, 1985), vol. 3, pp. 105–110.
39. National Oceanic and Atmospheric Administration, *Bathymetric charts of Hawaii to Midway* (National Ocean Survey, U.S. Department of Commerce, Washington, DC, 1981).
40. H. W. Menard, *Science* **220**, 913 (1983).
41. B. U. Haq, J. Hardenbon, P. R. Vail, *ibid.* **235**, 1156 (1987).
42. J. E. Hoffmeister and H. G. Multer, *Geol. Soc. Am. Bull.* **75**, 353 (1964).
43. J. E. Bardach, *Science* **133**, 98 (1961).
44. D. W. Kinsey, thesis, University of Hawaii, Honolulu (1979).
45. L. Montaggione, *Ann. S. Afr. Mus.* **71**, 69 (1976).
46. J. D. Milliman and K. O. Emery, *Science* **162**, 1121 (1968).
47. K. J. Hsu and E. L. Winterer, *J. Geol. Soc. Lon.* **137**, 509 (1980).
48. S. O. Schlanger, H. C. Jenkins, I. Premoli-Silva, *Earth Plan. Sci. Lett.* **52**, 435 (1981).
49. D. Q. Bowen, *Nature* **238**, 621 (1980).
50. J. I. Tracey, Jr., and H. S. Ladd, in *Proceedings of the Second International Coral Reef Symposium*, A. M. Cameron *et al.*, Eds. (Great Barrier Reef Committee, Brisbane, Australia, 1974), pp. 537–550.
51. T. Spenser, *Coral Reefs* **4**, 59 (1985).
52. J. F. Campbell, *Geo-Mar. Lett.* **6**, 139 (1986).
53. T. A. Davies, P. Wilde, D. A. Clague, *Mar. Geol.* **13**, 311 (1972).
54. B. Parsons and J. G. Sclater, *J. Geophys. Res.* **82**, 803 (1977).
55. W. C. Pitman III, *Geol. Soc. Am. Bull.* **89**, 1389 (1978).
56. We thank S. V. Smith, I. Macintyre, T. Jones, and J. Winterer for reading the manuscript and offering helpful suggestions. R.W.G. thanks the National Sea Grant Program (grant NA-81AA-D-00070) and the State of Hawaii, Office of Ocean Resources, Department of Business and Economic Development for financial support of this research. D.E. was supported by the Office of Naval Research and the National Science Foundation. Hawaii Institute of Marine Biology contribution No. 758, Department Business Economic Development contribution No. 72.

31 August 1988; accepted 22 December 1988

The Scanning Ion-Conductance Microscope

P. K. Hansma, B. Drake, O. Marti,* S. A. C. Gould, C. B. Prater

A scanning ion-conductance microscope (SICM) has been developed that can image the topography of nonconducting surfaces that are covered with electrolytes. The probe of the SICM is an electrolyte-filled micropipette. The flow of ions through the opening of the pipette is blocked at short distances between the probe and the surface, thus limiting the ion conductance. A feedback mechanism can be used to maintain a given conductance and in turn determine the distance to the surface. The SICM can also sample and image the local ion currents above the surfaces. To illustrate its potential for imaging ion currents through channels in membranes, a topographic image of a membrane filter with 0.80-micrometer pores and an image of the ion currents flowing through such pores are presented.

The family of scanning probe microscopes (*1–4*) is broadening the frontiers of surface imaging. These microscopes scan various sharp probes over samples to obtain surface contours—in some cases at the atomic scale (*2*). We report results from the SICM. It is designed specifically for biology and electrophysiology in that it can image soft nonconductors (such as membranes) that are covered with an electrolyte.

A schematic view of the SICM is shown in Fig. 1. A micropipette is filled with electrolyte and lowered through a reservoir of electrolyte toward an insulating sample surface while the conductance between an electrode inside the micropipette and an electrode in the reservoir is monitored. As the tip of the micropipette approaches the surface, the ion conductance decreases because the space through which ions can flow is decreased. The micropipette is then scanned laterally over the surface while a feedback system raises and lowers the micropipette to keep the conductance constant. The path of the tip follows the topography of the surface.

Department of Physics, University of California, Santa Barbara, CA 93106.

*Present address: Institut für Quantenelektronik, ETH Hönggerberg, HPT, CH-8093 Zürich, Switzerland.

Preliminary experiments were performed in our lab in 1986 by J. Saad and G. Tarleton (*5*). They were able to measure the topography of machined plastic pieces using an eyedropper as a probe. These experiments were not pursued further because the scan ranges then available with our microscopes (*6*) were not much larger than the openings in available micropipettes.

However, x,y,z piezoelectric translators with larger scan ranges are now available, and microscope design has evolved enough that experimentation with various scanning probes is relatively easy. The pipette of the SICM is brought near the surface with two fine screws that are adjusted by hand while the separation is monitored with an optical microscope (*7*). A third fine screw that is driven with a stepper motor (*7*) brings the pipette within range of a single-tube x,y,z piezoelectric translator (*8*). This translator has a 9.3-μm lateral range and a 3.0-μm vertical range (*9*).

The micropipettes for early experiments were made from 1.5-mm outer diameter (OD), 0.75-mm inner diameter (ID) Omega Dot (*10*) capillary tubing. Later versions were made with similar tubing (*11*) on a Brown-Flaming (*12*) puller. Although these pipettes are designed for measurement of intracellular potentials and patch clamping, similar micropipettes have been used in other scanning probe microscopes, namely the near-field scanning optical microscope and the micropipette molecule microscope (*3*). We estimated our micropipette tip diameters with a nondestructive bubble pressure method developed by Mittman *et al.* (*13*).

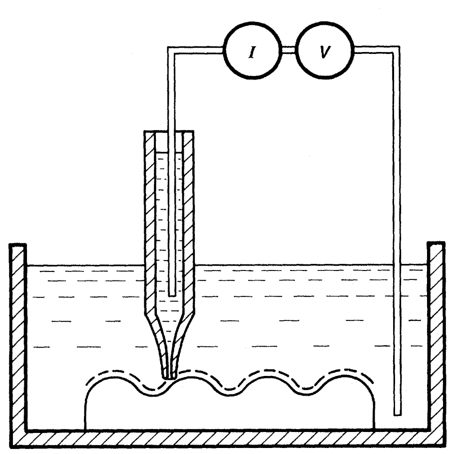

Fig. 1. The SICM scans a micropipette over the contours of a surface by keeping the electrical conductance through the tip of the micropipette constant by adjusting the vertical height of the probe.

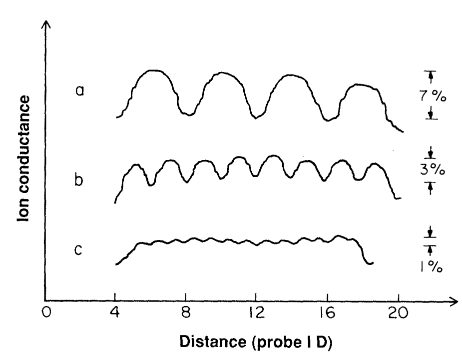

Fig. 2. Resolution test for the SICM. A pipette with an ID of 0.71 mm and an OD of 1.00 mm was scanned at constant height over three grooved plastic blocks with spacing of (a) four times, (b) two times, and (c) the same as the ID of the pipette. A 0.1M NaCl solution covered the blocks and filled the pipette. Note that even the grooves spaced by the ID of the pipette could be resolved.